Discriminative and quantitative analysis of norepinephrine and epinephrine by Surface Enhanced Raman Spectroscopy with gold nanoparticle suspensions

Antoine Dowek, Marion Berge, Patrice Prognon, François-Xavier Legrand, Eric Larquet, Ali Tfayli, Laetitia Minh Mai Lê, Eric Caudron

Discriminative and quantitative analysis of norepinephrine and epinephrine by Surface Enhanced Raman Spectroscopy with gold nanoparticle suspensions

Antoine Dowek[1,2], Marion Berge[1,2], Patrice Prognon[1,2], François-Xavier Legrand[3], Eric Larquet[4], Ali Tfayli[2], Laetitia Minh Mai Lê[1,2], Eric Caudron[1,2]

[1]Service de Pharmacie, Hôpital européen Georges Pompidou, APHP.Centre Université-Paris, 20 rue Leblanc, 75015 Paris, France.

[2]Université Paris-Saclay, Lipides, Systèmes Analytiques et Biologiques, 92296, Châtenay-Malabry, France.

[3]Université Paris-Saclay, CNRS, Institut Galien Paris Sud, 92296, Châtenay-Malabry, France.

[4]Laboratoire de Physique de la Matière Condensée (LPMC), Ecole Polytechnique, CNRS, Institut Polytechnique de Paris, 91128 Palaiseau, France

Corresponding author: Antoine Dowek, antoine.dowek@universite-paris-saclay.fr

Abstract:

Surface enhanced Raman spectroscopy (SERS) is a powerful analytical technique capable of increasing the Raman signal of an analyte using specific nanostructures. The close contact between those nanostructures, usually suspension of nanoparticles, and the molecule of interest produces an important exaltation of the intensity of the Raman signal. Even if the exaltation leads to an improvement of Raman spectroscopy sensitivity, the complexity of SERS signal and the numbers of parameters to be controlled conduct to use SERS for detection rather than quantification.

The aim of this study was to develop a robust discriminative and quantitative analysis in accordance with pharmaceutical standards. In this present work, we develop a discriminative and quantitative analysis based on the previews optimized parameters by design of experiments fixed for norepinephrine (NOR) and extended to epinephrine (EPI) which are two very close structure neurotransmitters. Studying the short evolution of the Raman signal intensity over time coupled with chemometric tools allowed to identify the outliers and to remove them from the data set. The discriminant analysis showed an excellent separation of EPI and NOR. The comparative analysis of the data showed the superiority of the multivariate analysis after logarithmic transformation. The quantitative analysis allowed the development of robust quantification models from several gold nanoparticle batches with limits of quantification obtained were 32 µg/mL for NOR and below 20 µg/mL for EPI even though no Raman signal is observable for such concentrations.

This study improves SERS analysis over ultrasensitive detection for discrimination and quantification using handled Raman spectrometer.

Keys words: Surface Enhanced Raman Spectroscopy, Gold nanoparticles, Quantitative analysis, Discriminative analysis, Mathematical design, neurotransmitters

Graphical abstract:

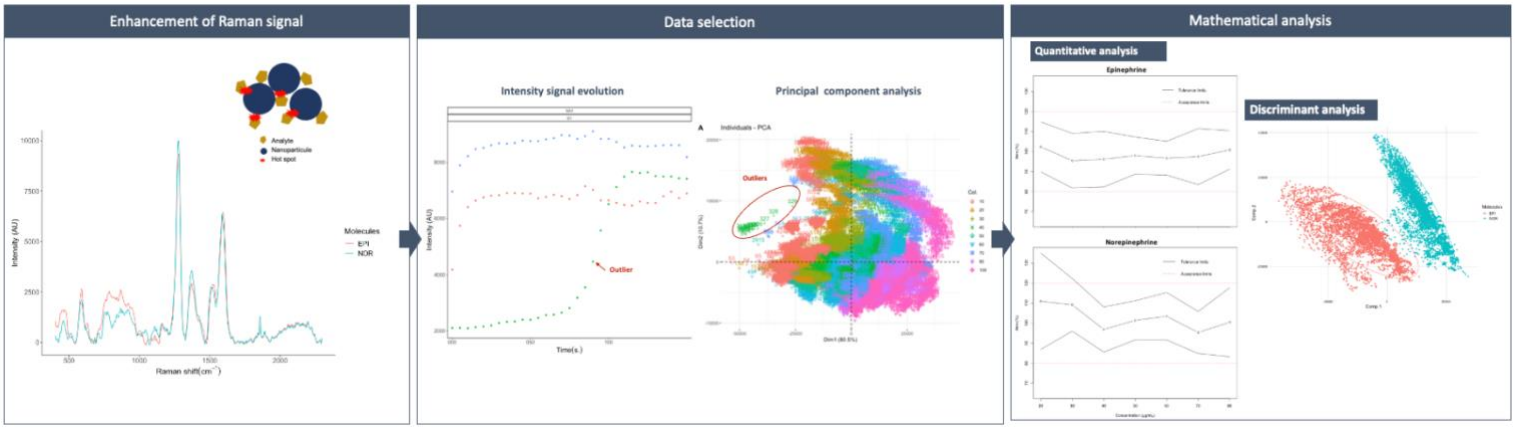

Raman spectroscopy is a promising technique capable of analyzing a large range of components by recording the vibrational signature of the molecule of interest (1). It had already been used in several fields such as the pharmaceutical field (2–7). However, due to lack of sensitivity, the technique to analyze molecules with concentrations of about mg/mL only. To overcome this lack of sensitivity, surface enhanced Raman spectroscopy (SERS) has been applied as a promising technique capable of enhancing Raman signal using metallic nanostructures called SERS substrates (8). This enhancement could reach 10^{14} (9) in very specific conditions. More commonly, the amplification of Raman signal in SERS is between 10^4 to 10^8, which remains a significant improvement in the sensitivity of Raman signal. This technique has therefore developed rapidly as an ultrasensitive detection technique, particularly in the pharmaceutical field, for which a review of literature has recently been published (10). However, this enhancement is very complex to master. Indeed, it requires a close and stable interaction between the SERS substrate and the molecule of interest. It involves many parameters such as the nature of the SERS substrate (metal, support, geometry, synthesis reproducibility), the interaction between the SERS substrate and environmental matrices, and the interaction between the SERS substrate and the analyte. For this reason, many studies focus only on SERS detection and fewer studies focus on quantification, which remains a particularly challenging field of applications (11). Current research in SERS tends to focus on the use of more complex nanoparticles (NPs) to improve detection sensitivity and to answer the needs of biological analysis rather than building robust quantitative models that can be used routinely. Only a very small number of studies have described quantification using gold or silver colloidal nanoparticles. Most of them are built with one batch of NPs using univariate (12–14) or multivariate analysis (15). A few deal with several batches of NPs using univariate (16,17) or multivariate (18) models.

This study aims at mastering the use of spherical gold NPs in suspensions synthesis coupled with experimental conditions previously optimized by design of experiments to develop efficient discriminative and quantitative models from several batches of colloidal NPs and by testing different mathematical approaches.

The first parameter to control for reproductible analysis in SERS is the substrate synthesis. Most documented synthesis are metallic NPs in suspension (19), which are known since the 1950s thanks to the Turkevich (20) synthesis for AuNPs and later Lee & Meisel (21) for silver NPs. These syntheses are well documented but controlling size and shape

reproducibility is still a challenge (19,22,23). The precise control of the synthesis allowing a reproducible size and geometry of the nanoparticles has a major impact on the amplification power in SERS (24). The second most important parameter is the interaction between NPs and the analyte which implies controlled experimental conditions (25) and being able to reproduce the same interaction from one experiment to an another, specifically controlling the NPs surface (charge, molecule, functionalization) and considering affinity between NPs and the analyte. Finally, to deal with spectral information contained in SERS spectra and link it to discrimination or quantification analysis, data analysis and the use of chemometrics tools (26–29) is needed.

The aim of this work is to construct a large data set for the analysis of two major neurotransmitters in our organism: NOR and EPI, which are two molecules of very close structure, to perform discrimination of the two analytes and quantitative analysis at low concentrations. If a few studies on the detection of catecholamines exist by SERS (30,31), it remains challenging to explore their quantification (32). This work focuses specifically on how to deal with important amount of data in SERS data processing. The first step was to select the relevant data set by discarding the outliers. Then, the goal was to build different mathematical models capable of reducing the variability of the signal in order to obtain the best predictive models in discrimination and quantification. Finally, the data was put in accordance with French pharmaceutical standards (33) in order to promote SERS as a reliable daily routine technique.

Experimental section:

Chemicals

Potassium gold (III) chloride ($KAuCl_4$, purity > 98%, European Pharmacopeia quality) was obtained from Sigma-Aldrich (Saint – Louis, USA). Trisodium citrate dihydrate ($C_6H_5Na_3O_7$, $2H_2O$, European Pharmacopeia quality, 98 %) was purchased from VWR Chemicals (Leuven, Belgium). The pharmaceutical formulation of EPI at 1 mg/mL was obtained from Aguettant (Lyon, France) and NOR 2 mg/mL was acquired from Mylan (Paris, France). Aggregating agent solution have been directly diluted from hydrochloric acid 1 M (HCl, European Pharmacopeia quality, VWR Chemicals, Fontenay-sous-Bois, France). Ultra-pure water was generated from Milli-Q system (Millipore, Bedford, MA, USA). Aqua Regia used to clean up glassware was prepared by mixing 3 volumes of hydrochloric acid 37 % (HCl,

European Pharmacopeia quality, VWR Chemicals, Fontenay-sous-Bois, France) and 1 volume of nitric acid 65 % (HNO_3, suprapur, Merck, Darmstadt, Germany).

Synthesis and characterization of gold nanoparticles

Gold nanoparticles (AuNPs) in suspension were described as easier to control than those with other metals. AuNPs were synthetized by reducing gold adding citrate as a reductant and stabilizing agent following the Turkevich method (20). According to Shin et al. (22), the ratio between citrate and gold was modified and fixed at five to promote better homogeneity in size and shape of gold nanoparticles. Chlorohydric acid was then used as an aggregation agent by reduction of charge at the nanoparticle surface.

Briefly, 11.2 mg of $KAuCl_4$ were dissolved in ultra-pure water and heated to 80°C while a solution of trisodium citrate at 1% were prepared. Then KAuCl4 solution were heated to 140°C, citrate solution was added at boiling point in one time. The mixture was under reflux at 900 rpm during 15 min, then the suspension was cooled at room temperature during one hour before analysis. All glass materials were washed with an acidic solution of aqua regia to dissolve traces of metal.

Three different batches of AuNPs suspensions (SA1, SA2, SA3) were prepared and characterized by transmission electronical microscopy (TEM), spectral UV analysis (UV), dynamic light scattering (DLS).

Drops of 5 µL of AuNPs samples were deposited onto 200 mesh freshly glow-discharged copper grids covered by a thin carbon film (Agar S160) for TEM observation. After adsorption and drying, the grid was mounted on a side-entry single tilt specimen holder and inserted in the microscope. The gold particles were observed using a Thermo-Fisher Themis 300 transmission electron microscope equipped with a Cryo-Twin (C-Twin) objective lens (Cs: 2.7 mm, Cc: 2.7 mm, focal length: 3.5 mm), using a XFEG electron gun (extraction voltage 4350 V, gun lens 3, emission current 320.2 µA) at an accelerating voltage of 300 kV, with the following illumination conditions: spot size 5, 2000 µm condenser C1 aperture, 150 µm condenser C2 aperture and no motorized objective aperture was inserted. Images were recorded with a magnification of x 58,000 on a Thermo-Fisher 4096 x 4096 pixels BM-Falcon III EC CMOS - DDE camera for a -50 nm to -300 nm defocus range. The pixel size of each image is 0.187 x 0.187 nm.

UV–visible spectra from 300 nm to 800 nm of the AuNPs suspension were recorded using a Varian Cary 50 UV–Vis (Agilent, Les Ulis, France) with one cm path length plastic

cells and ultra-pure water as reference sample. Based on UV spectra, the maximum wavelength (λmax) was determined to characterize the size of the nanoparticles for each AuNPs batch.

The hydrodynamic diameter of particles was determined at 25 °C by DLS using a Zetasizer Nano ZS 90 (Malvern Instruments, Malvern, UK) operating at fixed scattering angle at 90°. Measurements were performed in disposable 4 mL cuvettes with 1 cm optical pathway and four optical faces (Sarstedt, Marnay, France) containing an appropriate volume (1 mL) of sample. For each AuNPs batch, three samples were measured in triplicate for a total of nine measurements by batch.

Surface enhanced Raman spectroscopy condition

Spectra were acquired with the handled Metrohm Instant Raman Analyzer (MIRA, Metrohm, France) equipped with a 785 nm diode. Analyses were performed using the vial module at a focal length of 0.85 mm. The orbital raster scan (ORS) measured the signal at different points in the sample. SERS signals were acquired from 400 cm^{-1} to 2,300 cm^{-1} with a spectral resolution from 12 cm^{-1} to 14 cm^{-1}.

The SERS experiments corresponding to optimal conditions were conducted in a glass vial as follow: 135 µL of analyte were added to 465 µL of AuNPs suspension (ratio $V_{NPs}/V_{Analyte}$ = 3.5) for a final volume of 600 µL and vortexed for 5 sec. Then, 10 µL of HCl 0.7 M were added to the mixture and again vortexed for 5 sec. The samples were directly analyzed by MIRA Raman spectrometer. The acquisitions were performed for 3 sec every 8 seconds during 4 min corresponding to 31 spectra for each sample.

Data set construction

To construct performant quantification and discriminant models for each catecholamine (EPI and NOR), a large data set was acquired.

For each drug, experiments were done using three different batches of AuNPs (SA1, SA2, SA3). For each batch of NPS, analyses were performed with new drug preparation set for three consecutive days of analyses (G1, G2, G3), and prepared each day in triplicate (R1, R2, R3), including nine levels of concentration from 10 to 100 µg/mL. For EPI and NOR, a total of 486 samples (2 drugs, 3 batches of AuNPs suspensions x 3 days x 3 replicates x 9 concentrations) were analyzed for a total of 15,066 spectra (31 times of analysis per sample).

According to the guidelines of European Medicines Agency (EMA) for infrared spectroscopy analysis, data set was randomly divided by 9 series of data, defined as experiments acquired for one AuNPs batch during one day (SAXGY) in one calibration set (6 series, 2/3 of data) to construct the mathematical predictive model and evaluated cross validation error, and one validation set (3 series, 1/3 of data) independent from calibration data set in order to evaluate the predictive performances of the mathematical model.

Data analysis

Raman spectra are complex data to analyze, specifically in SERS analysis which induces variability of enhancement. The Raman signal can be disturbed by many parameters such as spurious diffusion, fluorescence, the structure of container, the size of particles in the suspension. To avoid these physical interactions, spectral pretreatments should be used. In this study, it was chosen to use few pretreatments in order to keep the structure of the original signal. Therefore, the baseline deviation was corrected by asymmetric least square regression (34) (second derivative constraint equal to 6) and smoothing was applied using Savitzky-Golay method (first order polynomic and a window size equal to 7) to reduce background noise. Moreover, logarithmic base ten transformation was also evaluated because spectral enhancement in SERS can induced spectral transformation and non-linear evolution of the Raman signal with concentration.

Firstly, principal component analysis (PCA) was used to visualize data dispersion, and to individualize atypic results. PCA is an exploratory data analysis tool (35) that creates a new axis called principal components (PC) trying to catch for each component the maximum of variability. PCA is an unsupervised tool based on orthogonal reduction of dimension. Therefore, it's a practical technique capable of exploring a large dataset.

In order to construct the best prediction model, several approaches were tested beginning with a usual approach based on univariate linear regression, which correlates a single intensity of all spectra with the concentration of the analyte. Because Raman spectra are complex to analyze and contain a large amount of information, multivariate analysis was also performed. To develop a quantitative model of prediction, multivariate analysis able to include intensities mostly correlated to concentration were explored such as partial least square regression (PLSR) (36). PLSR consists in constructing the regression model as shown in Equation 1 (developed for logarithmic transformation too Equation 2), where Y is the response matrix (concentrations), X the matrix of predictors, B the matrix of coefficients and E the

residual error matrix. The goal is to construct new variables, called latent variables (LVs), which are linear combinations of initial variables that contain most of the variability and that best correlate to the response being studied. This technique is particularly appreciated in spectral data processing because it allows to get rid of collinearity phenomena and to visualize the most important spectral areas quickly and concisely, which represent the most weight in the construction of the model.

Equation 1General equation of PLS regression.

$$\mathbf{Y} = \mathbf{X}.\mathbf{B} + \mathbf{E}$$

Equation 2 PLS regression with logarithmic transformation.

$$\boldsymbol{log(Y) = log(X).B + E}$$

Alike for quantitative analysis, PLS was used for discriminant analysis (PLSDA) (37). Following the same principle as for PLSR, PLSDA is a linear classification model able to predict the class of new samples. Here, the response matrix Y is qualitative and is internally recoded. Each of the response categories are coded via an indicator variable. The PLS regression is then run as if Y was a continuous matrix. All data analysis process is sum up in Fig. 1.

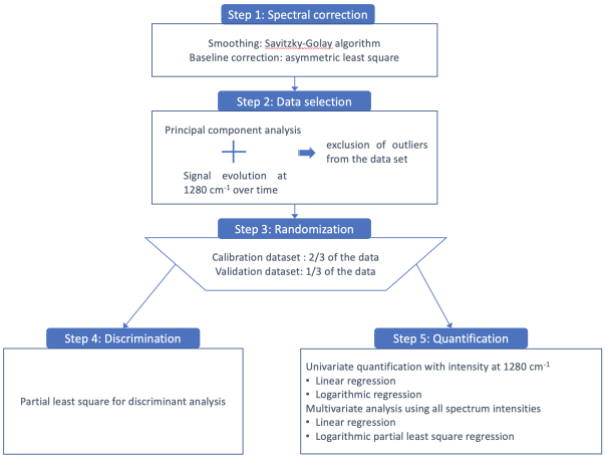

Fig. 1 Flow chart of data analysis process from spectral pretreatments to quantification and discrimination steps

In order to choose the mathematical models developed, different indicators were determined as correlation coefficient R^2 calculated to ensure the correlation between predictors and concentrations, root mean square error (RMSE, Equation 3) and mean absolute relative error (MARE,

Equation *4*) to compare prediction error calculated regardless the mathematical model used.

The root mean square error of cross-validation was calculated (RMSECV) for calibration data set by k-fold cross validation for groups of 20 (only for PLS regression). This parameter was used to determine the number of latent variables (LV) to be used in PLS models. This number was selected by permutation approach, which selected the lowest number of LVs for which no difference between two consecutive RMSECV were observed.

For validation data set root mean square error of prediction (RMSEP) was calculated to evaluate the robustness of the model. If the model is robust RMSEP should stay stable. Randomization for validation data set was done based on nine series of data defined as experiments acquired for one AuNPs batch during one day for example SA1G1 for a total 84 randomizations. The series used to construct accuracy profile with a 10 % ß error and acceptance limits set at 20 % was selected for the lowest RMSEP.

Equation 3 Root mean square error (RMSE); y_i represents real concentration of analyte and $\hat{y}_i$ the estimated concentration.

$$\mathbf{RMSE} = \sqrt{\frac{\mathbf{1}}{\mathbf{N}}\sum_{\mathbf{i=1}}^{\boldsymbol{N}}(\mathbf{y_i} - \hat{\mathbf{y}}_\mathbf{i})^\mathbf{2}}$$

Equation 4 mean absolute relative error (MARE); y_i represents real concentration of analyte and $\hat{y}_i$ the estimated concentration.

$$\mathbf{MARE} = \frac{\mathbf{1}}{\mathbf{N}}\sum_{\mathbf{i=1}}^{\boldsymbol{N}}\frac{|\mathbf{y_i} - \hat{\mathbf{y}}_\mathbf{i}|}{\mathbf{y_i}}$$

Results

Characterization of AuNPs suspensions

AuNPs suspensions were characterized by three complementary techniques which combined can be considered as a good estimation of AuNPs shape and size. Results of size estimation of NPs are summarized in Table 1.

TEM images (Fig. 2DLS characterization is illustrated in Fig. 3 A and B by correlation coefficients and by intensity-weighted size distribution for SA1, SA2, SA3. These characterizations show size homogeneity for each batch and similar size between batches. UV-

visible spectra between AuNPs batches is well superposed suggesting the homogeneity of NP suspension in the three batches (Fig. 3 C). The lambda at maximum absorbance is close for the three batches suggesting a good batch to batch size reproducibility. UV-visible Spectra are also thin revealing the good homogeneity in AuNPs size for each batch.

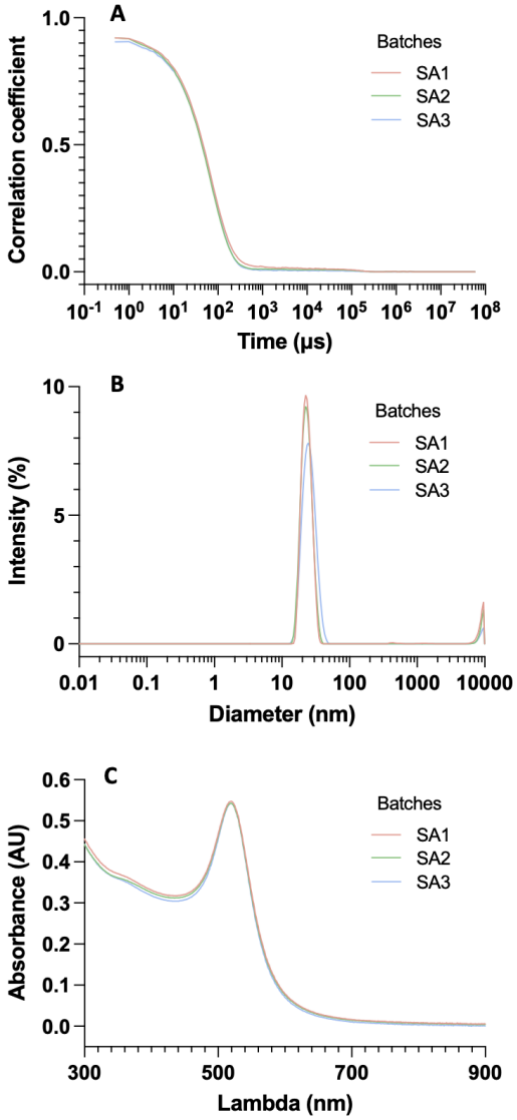

Fig. *3* Diffusion light scattering and UV-visible spectroscopy of AuNPs batches (SA1, SA2, SA3) A) correlation coefficient B) intensity-weighted size distribution C) UV-visible absorbance) should be the most relevant estimation of shape and size AuNPs because they allow direct visualization of the shape and size of AuNPs, for a mean size of 16.4 nm [16.2 - 16.6 nm] (n = 180). AuNPs size for each batch was calculated with 60 measurements measured using 10 TEM images.

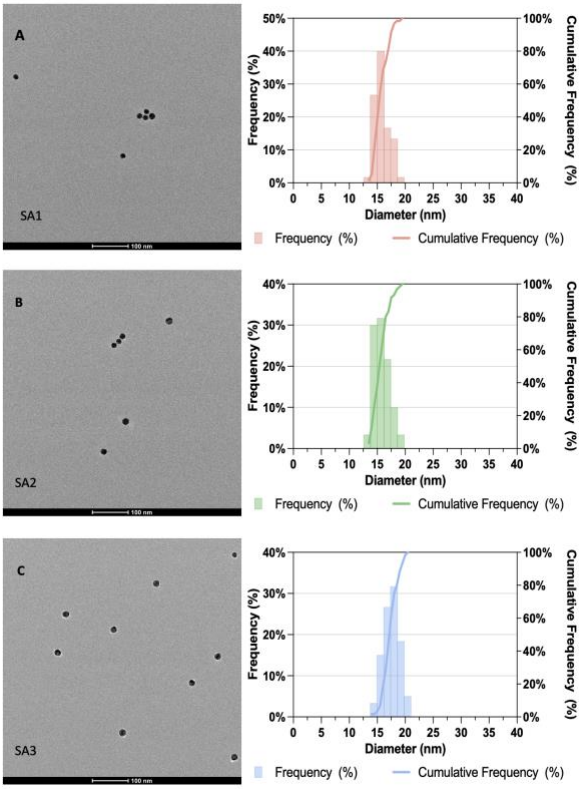

Fig. 2 Characterization of the three AuNPs batches by transmission electronic microscopy with on the right repartition of nanoparticle size (n = 60 for each batch) A) SA1, B) SA2, C) SA3

DLS characterization is illustrated in Fig. 3 A and B by correlation coefficients and by intensity-weighted size distribution for SA1, SA2, SA3. These characterizations show size homogeneity for each batch and similar size between batches. UV-visible spectra between AuNPs batches is well superposed suggesting the homogeneity of NP suspension in the three batches (Fig. 3 C). The lambda at maximum absorbance is close for the three batches suggesting a good batch to batch size reproducibility. UV-visible Spectra are also thin revealing the good homogeneity in AuNPs size for each batch.

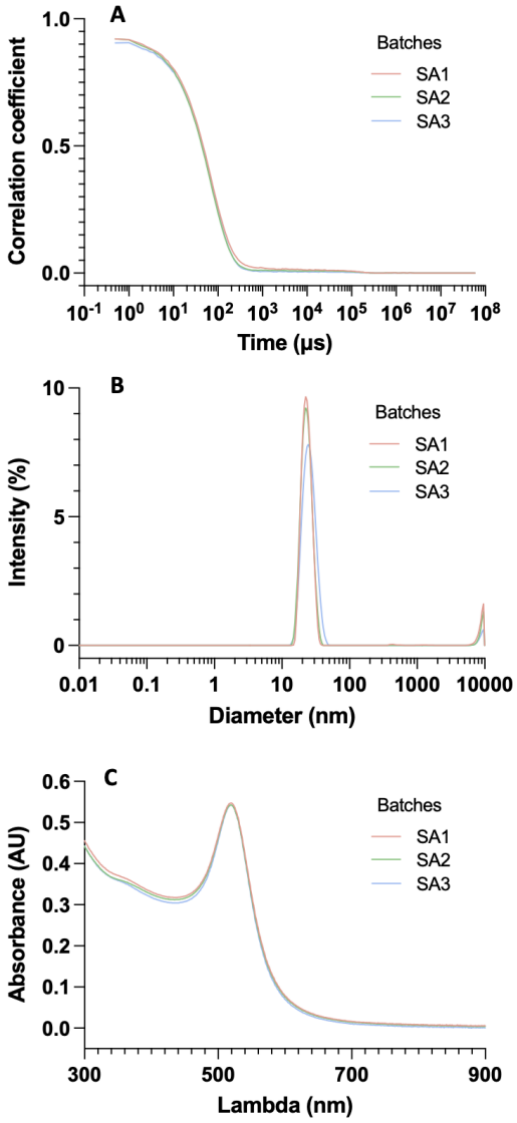

Fig. 3 Diffusion light scattering and UV-visible spectroscopy of AuNPs batches (SA1, SA2, SA3) A) correlation coefficient B) intensity-weighted size distribution C) UV-visible absorbance

Comparatively, DLS is always an overestimation of real size because measuring hydrodynamic diameter. Furthermore DLS confirmed the stability of AuNPs suspension calculating zeta potential for an average zeta at -34.3 mV allowing a repulsion capable ensuring NPs stability. Calculation of polydisperse index (PDI) by DLS confirmed the low dispersity of AuNPs batches with PDI of 0.15. All three techniques were concordant for spherical monodisperse AuNP suspensions.

Table 1 Size estimation of the three batches of gold nanoparticles SA1, SA2, SA3 by transmission electronical microscopy (TEM), ultraviolet spectroscopy (UV) and dynamic light scattering (DLS). The calculation of mean size is represented, included confidence interval at 95 % ([]) for TEM and DLS.

Batch of AuNPs suspension	TEM (nm) Mean [IC95%]	UV (nm)	DLS (nm) Mean [IC95%]
SA1	15.8 [15.5 - 16.1]	18.5	24.3 [24.0 – 24.6]
SA2	15.9 [15.6 - 16.2]	19.3	23.4 [23.2 – 23.6]
SA3	17.5 [17.2 - 17.8]	21.3	24.5 [24.4 – 24.7]

In conclusion, according to UV, DLS and TEM results, the AuNPs suspension synthesis technique was considered as reproductible, producing stable spherical gold NPs in suspension with homogeneous size of AuNPs (+/- 2 nm) and shape (standard deviation of 9.6 % calculated with TEM measurements).

Exploration of the data set

SERS enhancement

Firstly, Raman spectra were acquired directly from the commercial solution of EPI at 1 mg/mL and NOR at 2 mg/mL and for both drugs: no signal was observed. According to the condition of surface enhanced Raman spectroscopy describe in section "Surface enhanced Raman spectroscopy condition", an intense signal appeared (Fig. 4). According to several studies in Raman spectroscopy and SERS, Raman shifts were attributed (Table 2) to EPI, NOR (38,39), citrate or its derivatives (40,41) which can still be present in final AuNPs suspension.

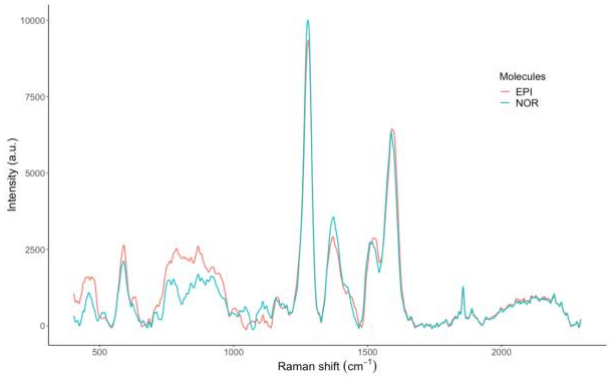

Fig. 4 SERS spectra (experimental conditions described in "Surface enhanced Raman spectroscopy condition") of epinephrine (EPI, red) and norepinephrine (NOR, blue) at 100 µg/mL (smoothing: Savitzky-Golay, baseline correction: asymmetric least square).

SERS spectra were compared with those obtained in Moody's studies (39,42,43) who acquired SERS spectra of several neurotransmitters in similar conditions (785 nm laser with AuNPs aggregated by HCl solution, or incorporated in agarose gel) and in Vander Ende work (44), who used polymeric aggregation in order to stabilize SERS signal. Principal Raman shifts presented here were also found in these studies.

Table 2 Relative intensities and attributions of main Raman shift observed in SERS spectra of NOR, EPI and citrate in gold nanoparticle suspensions.

Raman shift (cm^{-1})	Relative intensity	Chemical attribution	Molecule attribution
470	0.18	COO quenching	Citrate / derivative
590	0.28	CC=O stretching	NOR/EPI
630	0.11	COO deformation	Citrate / derivative
790	0.28	Ring breathing	NOR/EPI
870	0.29	C-COO stretching	Citrate / derivative
1000	0.08	C-O stretching	Citrate / derivative
1080	0.01	CCH bending	NOR/EPI
1168	0.09	CO stretching	NOR/EPI
1280	1.00	CO asymmetric stretching	NOR/EPI
1375	0.30	Symmetric COO	Citrate / derivative
1530	0.37	Asymmetric COO	Citrate / derivative
1593	0.74	CC aromatic stretching	NOR/EPI

SERS contact time

For all samples, 31 spectra were successively acquired to evaluate the impact of time on the aggregation process between AuNPs and the analyte and thus, SERS signal. The Fig. 5 (A.1 and B.1) represents the SERS signal evolution for the 1280 cm^{-1} intensity Raman shift for few experiments at 40 µg/mL. For most experiments, the SERS signal evolution increases for the first four measurements, followed by a slight stabilization and a slow decrease for the last measurements. For a few experiments, the evolution of the signal during the experiment was different. These experiments were listed and considered atypical. Parallelly, PCA were conducted to explore rapidly all data set.

For NOR dataset, PC1 (Fig. 5 A.2) which represented 81.4 % of total variance seems to be correlated to the concentration while PC2 (10 % of total variance) individualized a group of

samples identified as SA1G1R1 and SA1G1R3. These series also have a different evolution over time. Based on these two results, SA1G1R1 and SA1G1R3 (PCA score plot individualized by SAXGYRZ is available in supplementary information) were considered as outliers and were excluded from the data for qualitative and quantitative analysis.

For EPI, PC1 (Fig. 5 B.2) represented 80.5 % of the variance and seemed to be linked to the concentration of EPI, except for SA1G1R2 40 µg/mL. Likewise, the data SA1G1R2 40 µg/mL confirmed the data as outliers and excluded it for the rest of the analysis.

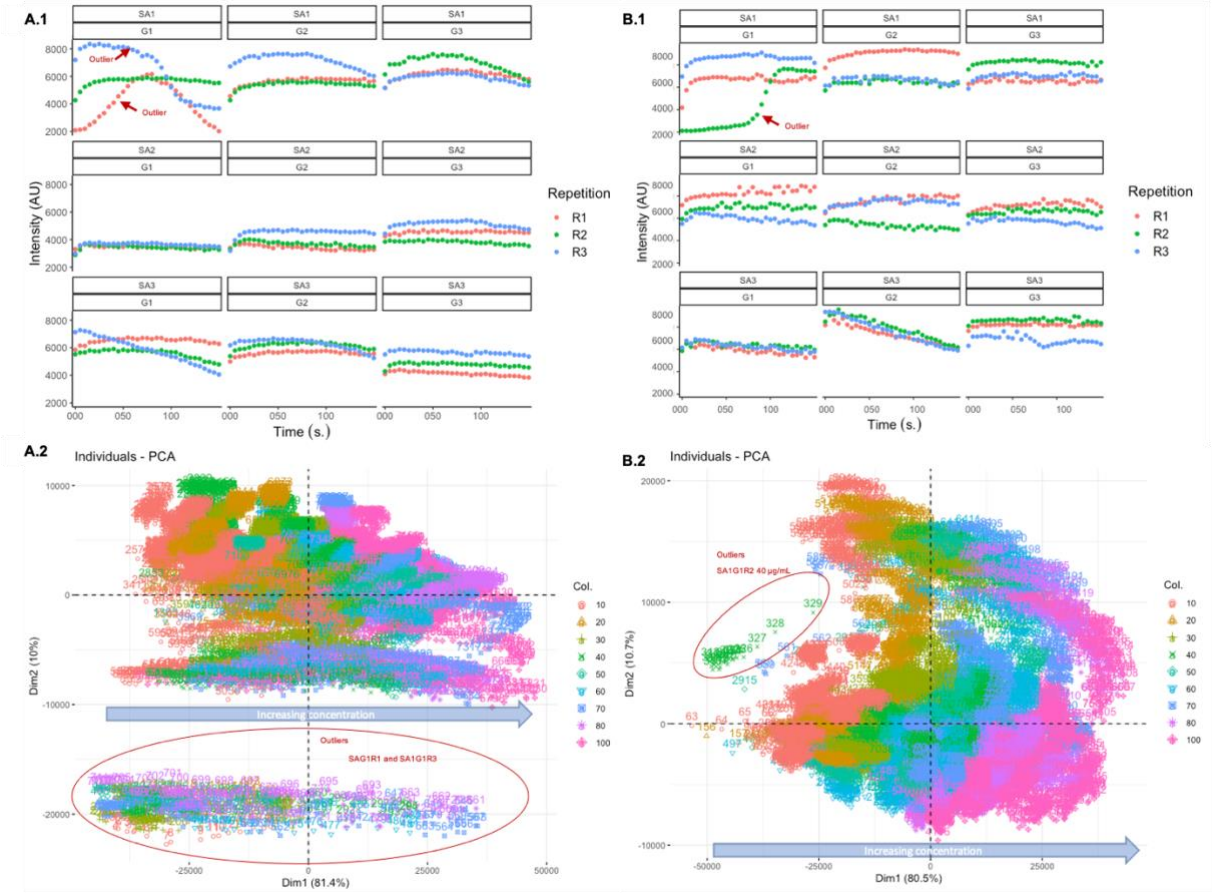

Fig. 5 Selection of outliers: A.1 Evolution of the SERS signal at 1280 cm^{-1}over the time for norepinephrine at 40 µg/mL, A.2 Principal component analysis for all norepinephrine spectra colored by concentration, B. Evolution of the SERS signal at 1280 cm^{-1}over the time for epinephrine at 40 µg/mL, B.2 Principal component analysis for all epinephrine spectra colored by concentration

For quantitative and discriminant analysis, all outliers identified by PCA and atypical evolution of signal over time was removed. Furthermore, high signal variations at 1280 cm^{-1} were observed on the first four measurements for every experiment suggesting a variability in SERS signal in the first seconds of the analysis. The first four data points were excluded from the analysis.

Discriminant analysis

The best PLS-DA models were obtained after ALS and SG pretreatments, for all experiments for NOR and EPI excluding outliers previously described (outliers for NOR: SA1G1R1, S1G1R3; for ADR: SA1GA1R2 40 µg/mL; acquisition time > 15 sec.).

Results are represented, as an example, in Fig. 6. for validation set: SA3G3, SA3G1, SA2G1. The first component determined which samples are NOR or EPI (Fig. 6 A.), while second component seems more linked to the concentration (Fig. 6 B.). Watching loadings (Fig. 6 C.) can define an area in spectra from 750 to 1000 cm^{-1} which has an important impact on molecule discrimination. This could be attributed to differences between primary or secondary amine group.

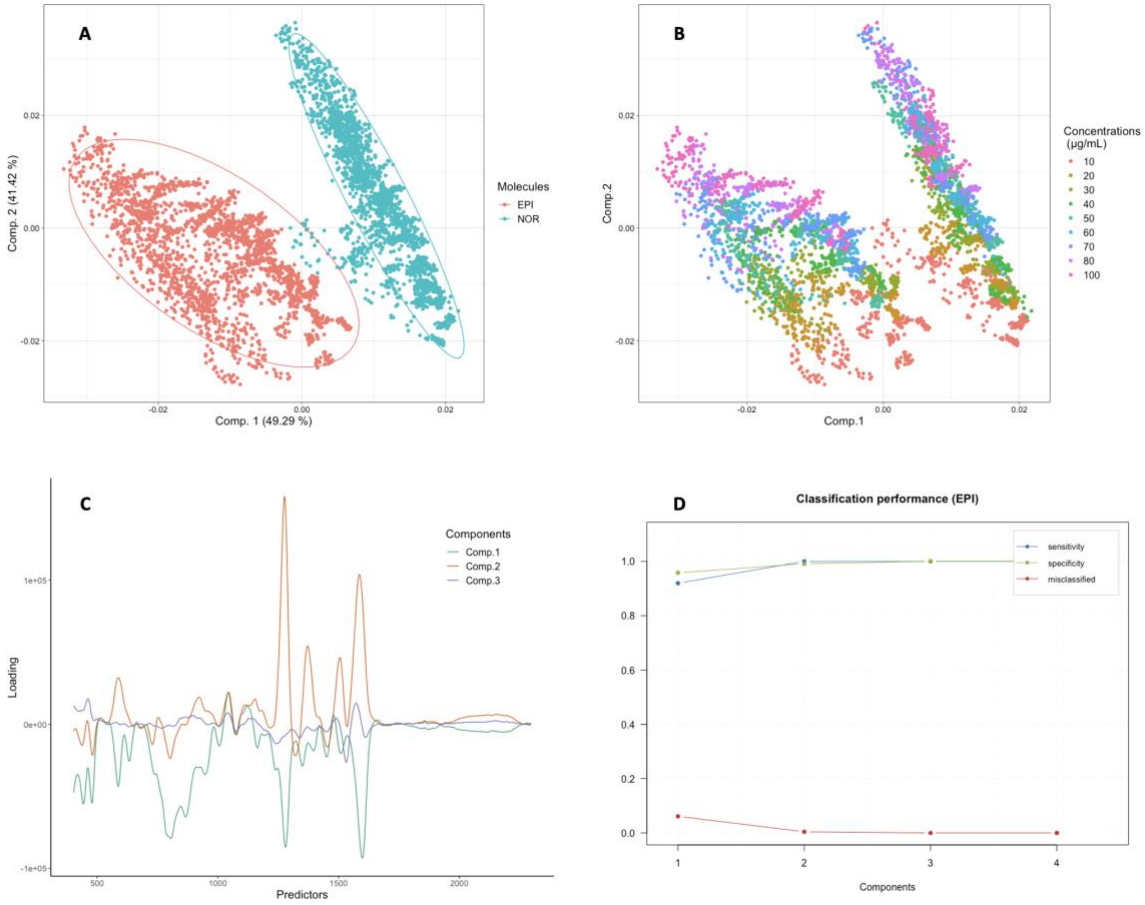

Fig. 6 Discriminant analysis, representation of the three first components. A: regrouping molecules, B: regrouping concentrations, C: loadings representation. D: performances of PLS-DA analysis, example for validation set: SA3G3, SA3G1, SA2G1

Using only three components, the confusion matrix gave an accuracy of 1, therefore 100 % of validation data set (SA3G3, SA3G1, SA2G1) (4,374 spectra) were assigned to the right class, i.e. the right molecule. Performances (Fig. 6 D.) were similar independently of

validation data set, for the 84 randomizations with sensitivity of 1, specificity of 1 and 0 misclassified. These experiments confirm the excellent specificity of Raman spectroscopy and prove the ability of SERS to be used to discriminate two neurotransmitters of very close structure.

Quantitative analysis

Univariate analysis at 1280 cm^{-1} was firstly evaluated based on the evolution of the most intense Raman shift linked to the catecholamines signal. The evolution of this shift as a function of analyte concentration is represented in Fig. 7 A for NOR spectra pretreated by ALS and SG at one time selected (75 sec). Because signal evolution of this Raman shift didn't seem linear, logarithmic to the base 10 transformation was also performed as shown in the Fig. 7 B.

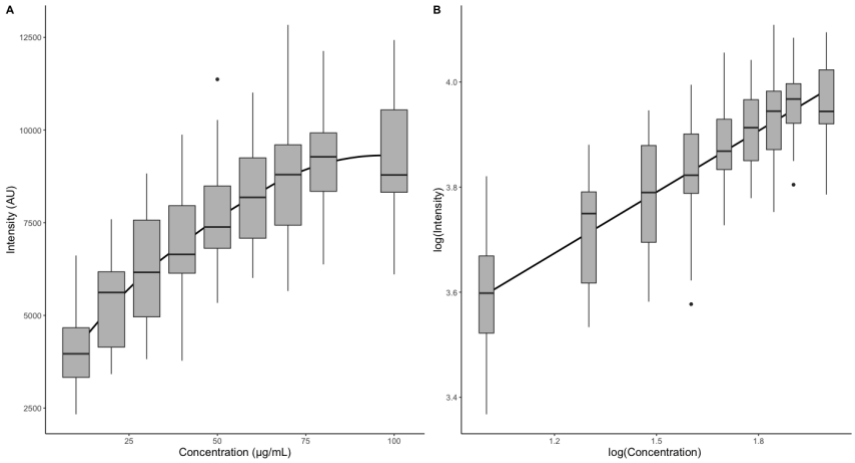

Fig. 7 Evolution of concentration as a function of intensity of 1280 cm^{-1} Raman shift (molecule: norepinephrine, time: 75 sec) A: pure, B: with logarithmic transformation

The highest concentration at 100 µg/mL but also the lowest concentration at 10 µg/mL associated to a large variability were removed from the data set to develop quantitative models. Therefore, the focus area has been reduced to 20 µg/mL to 80 µg/mL. Then multivariate analysis including all spectra intensities was performed, using PLS regression, with or without logarithmic transformation. In Table 3, are presented the main results of prediction indicators from all 84 randomizations. The number of latent variables selected by permutation algorithm were comprised between 14 and 16 for all randomizations.

Table 3 Comparison of mean results for 84 randomizations of the data set of R^2, root mean square error of prediction (RMSEP), mean absolute relative error (MARE) calculated for univariate or multivariate and with or without logarithmic transformation.

Molecule	Model	Y = X.B + E	log(Y) = log(X).B +E

		R^2	RMSEP (µg/mL)	MARE (%)	R^2	RMSEP	MARE (%)
EPI	Univariate at 1280 cm^{-1}	0.48	14.94	30	0.54	0.14	26
	Multivariate from 400 to 2300 cm^{-1}	0.95	5.47	11	0.96	0.06	9.1
NOR	Univariate at 1280 cm^{-1}	0. 40	16.06	34	0.50	0.15	29
	Multivariate from 400 to 2300 cm^{-1}	0.91	7,27	14	0.95	0.06	10

Regarding results of predictive indicators, multivariate analysis was preferred, comparison of ER and R^2 between logarithmic and non-logarithmic models are presented in Fig. 8 for EPI and Fig. 9 for NOR.

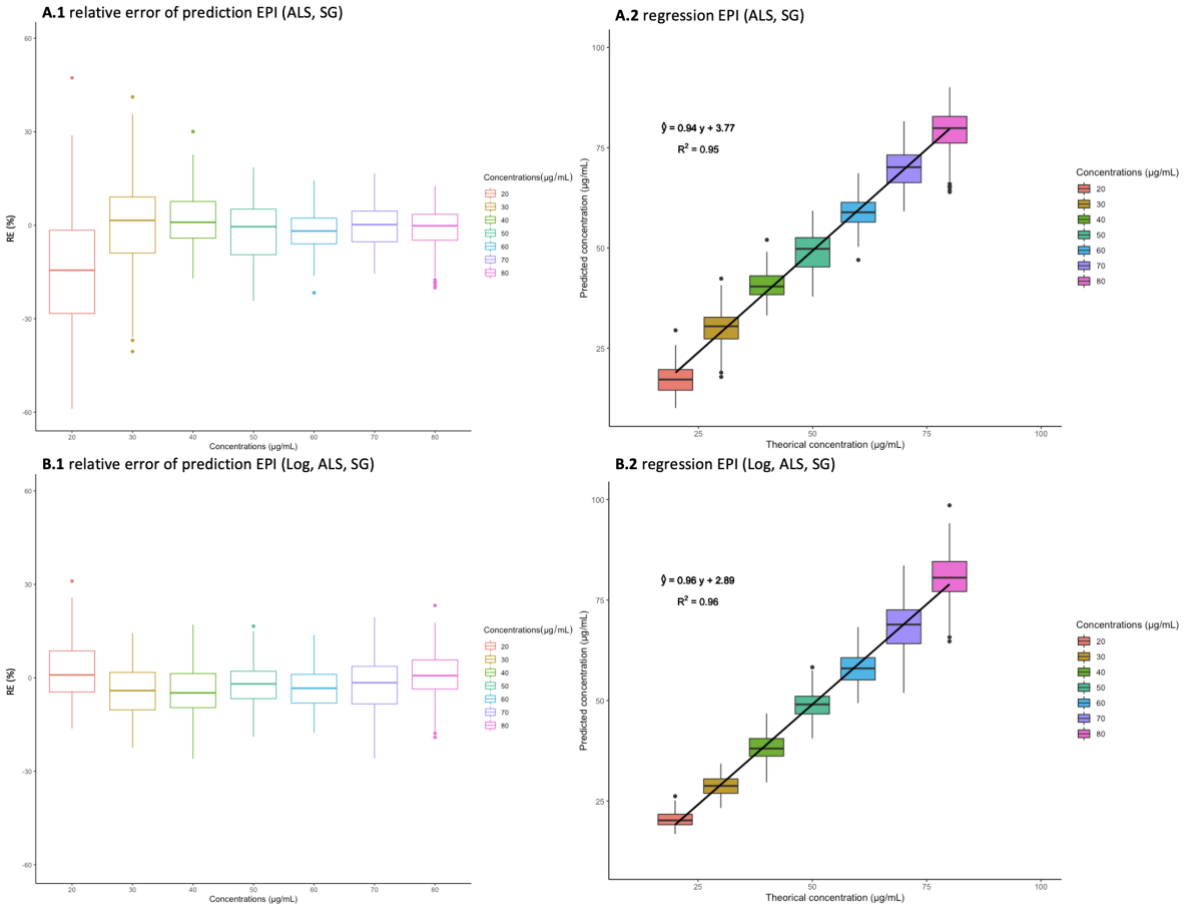

Fig. 8 Evolution of relative error for each concentration level and regression curve between predicted and theorical concentrations for epinephrine (EPI) with (B.1, B.2) and without logarithmic (A.1, A.2) transformation for multivariate analysis

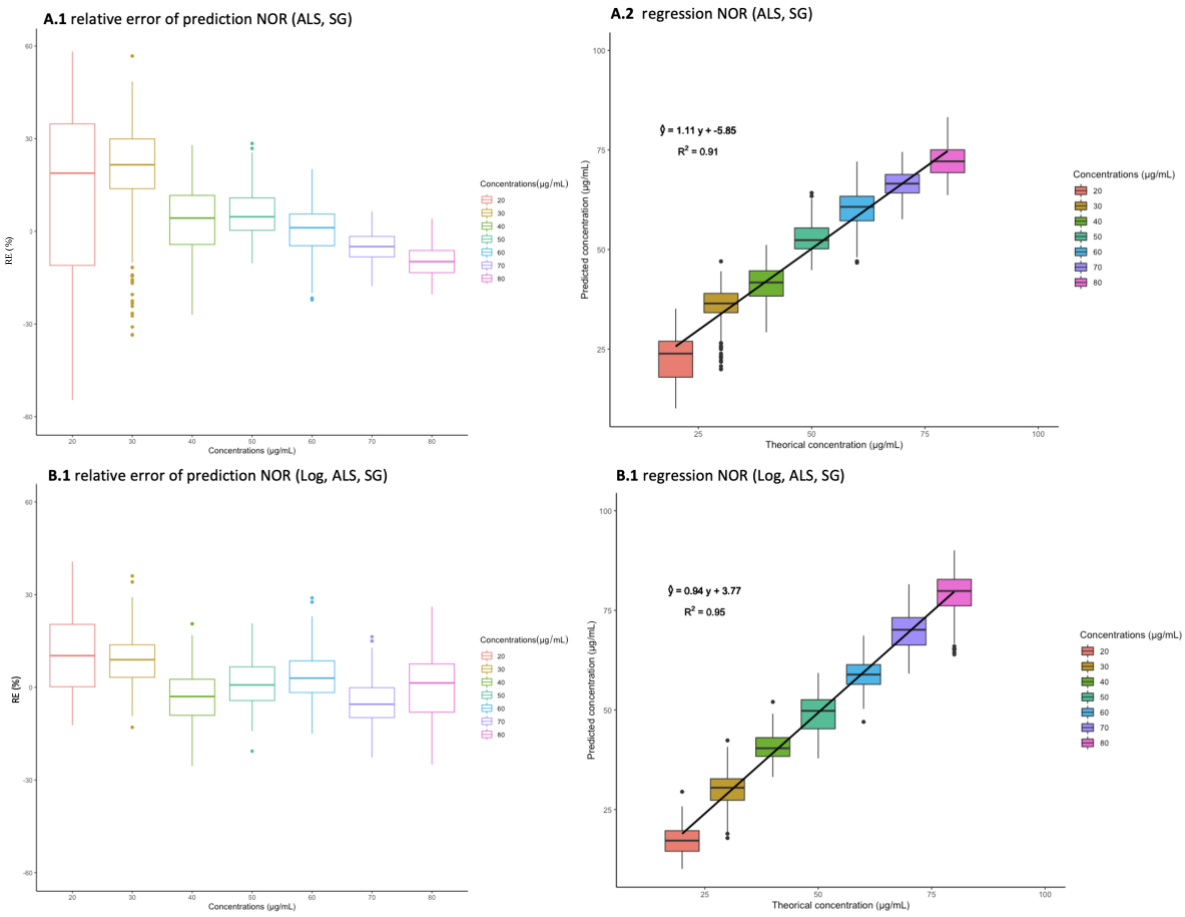

Fig. 9 Evolution of relative error for each concentration level and regression curve between predicted and theorical concentrations for norepinephrine (NOR) with (B.1, B.2) and without logarithmic (A.1, A.2) transformation for multivariate analysis

The dispersity of RE was higher for lowest concentrations with both approaches. An improvement of RE values was noticed for logarithmic transformation. The regression curve showed a good agreement between theorical and predicted concentrations with a R^2 superior to 0.9. The logarithmic model reduced RE for every level of concentration.

Based on these results, multivariate analysis with logarithmic transformation was used to build an accuracy profile, the validation data set was chosen for the lowest RMSEP i.e. data from SA1G3, SA2G1, SA2G3 for NOR and SA1G2, SA2G2, SA3G1 for EPI to validate the calibration model. Accuracy profiles constructed from these datasets are presented below Fig. ***10***.

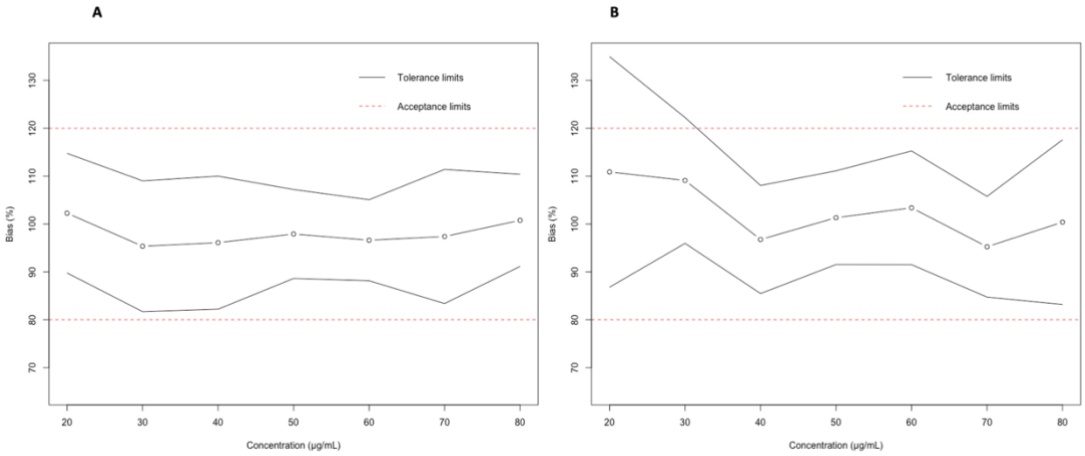

Fig. 10 Accuracy profiles of epinephrine (A) and norepinephrine (B), acceptance limits fixed to 20 %, tolerance limits fixed for a ß error of 10 %

Low limits of quantification (LLOQ) were determined directly from these profiles as the lowest concentration included between acceptance limits. LLOQ was equal to 32 µg/mL for NOR and 20 µg/mL for EPI.

Discussion

The aim of this study was to develop a robust discriminative and quantitative mathematical model for two drugs of interest: EPI and NOR. The focus on data selection and mathematical design aimed at trying to reduce lack of reproducibility induced by experimental variability of SERS signal.

For data selection, monitoring the evolution of the signal of the most intense Raman shift as a function of contact time should probably be the reflect of aggregation between AuNPs and the analyte. For a few seconds the signal increased and highlighted the interaction between these two components, then a slight stabilization was observed before a decrease of the signal, probably due to the beginning of sedimentation, showing the limits of aggregation by HCl. In some cases, the aggregation process takes place in an uncontrolled way and leads to an atypical evolution of the signal as a function of the contact time which can explain the outliers. These observations suggest that the evolution of the signal over time can define if a SERS experiment succeeded or not. The identification of outliers was very important for the construction of efficient quantitative models and atypical samples should then be removed for further analysis.

The discriminant analysis confirmed the specificity of Raman spectroscopy and so SERS. Few pretreatments and components were however needed to perform robust discrimination for the two molecules studied which only differ by one methyl group.

Mathematical design clearly showed the superiority of multivariate approach to deal with spectral data and greatly improved predictors. The important number of LVs selected by permutation can be explained by the large number of variabilities included in this dataset: several AuNPs batches, days, batches of drugs, level of concentrations, times of acquisition. Quantification was better for EPI than for NOR which may be explained by the important number of outliers removed from NOR dataset (total dataset of 5103 for EPI against 4671 for NOR). Other hypothesis could be that differences observed in 750-1000 cm^{-1} area may affect quantification performances. Observation of relative error by level of concentration clearly showed the impact of logarithmic transformation at every level of concentration. Quantitative performances demonstrate that SERS can be used as a validated technique for quantification if experimental conditions are controlled, and appropriate mathematical transformation is performed. The next step will be to master analyte and SERS substrate interaction in order to reach higher sensitivity.

Conclusion

In this study, we firstly succeeded in synthetizing controlled spherical gold nanoparticles in suspension and validating their homogeneity in shape and size according to TEM, UV and DLS. Then we clearly demonstrated the power of SERS in quantification and discriminant analysis with a handled Raman spectrometer. The specificity of SERS was highlighted with a discriminant analysis capable of perfectly separating two molecules of very close structures. Then we succeeded in quantifying a range of concentrations from 20 to 80 µg/mL for EPI and from 32 to 80 µg/mL for NOR with robust criteria, by firstly selecting experimental conditions by design of experiments and then applying logarithmic transformation to linearize our data before performing PLS regression. Performances should be improved by controlling more precisely the aggregation phenomenon and probably using nanostructures capable or further enhancing Raman intensity.

Declarations:

Conflicts of interests/Competing interests:

The authors declare no conflicts of interest.

Funding:

This work has been supported by the Fondation ARC pour la recherche.

Acknowledgments:

The authors would like to acknowledge financial support for Nan'eau microscope from Ecole Polytechnique, IDEX Paris-Saclay, Equipex Morphoscope 2 and DGA. They also thank the "Centre Interdisciplinaire de Microscopie électronique de l'X" (CIMEX) for the TEM images. Finally, they are grateful to the Fondation ARC (French foundation for cancer research) for the financial support to Marion Berge.

References

1. Michelet A, Boiret M, Lemhachheche F, Malec L, Tfayli A, Ziemons E. Utilisation de la spectrométrie Raman dans le domaine pharmaceutique. STP Pharma Prat. 2013;23(2):97-117.
2. Lê L, Berge M, Tfayli A, Prognon P, Caudron E. Discriminative and Quantitative Analysis of Antineoplastic Taxane Drugs Using a Handheld Raman Spectrometer. BioMed Res Int. 3 juill 2018;2018:1-7.
3. Shende C, Smith W, Brouillette C, Farquharson S. Drug Stability Analysis by Raman Spectroscopy. Pharmaceutics. déc 2014;6(4):651-62.
4. Parachalil DR, McIntyre J, Byrne HJ. Potential of Raman spectroscopy for the analysis of plasma/serum in the liquid state: recent advances. Anal Bioanal Chem. 1 avr 2020;412(9):1993-2007.
5. Lê L, Berge M, Tfayli A, Baillet Guffroy A, Prognon P, Dowek A, et al. Quantification of gemcitabine intravenous drugs by direct measurement in chemotherapy plastic bags using a handheld Raman spectrometer. Talanta. 1 mai 2019;196:376-80.
6. Mansouri MA, Sacré P-Y, Coïc L, De Bleye C, Dumont E, Bouklouze A, et al. Quantitation of active pharmaceutical ingredient through the packaging using Raman handheld spectrophotometers: A comparison study. Talanta. 15 janv 2020;207:120306.
7. Lê LMM, Berge M, Tfayli A, Zhou J, Prognon P, Baillet-Guffroy A, et al. Rapid discrimination and quantification analysis of five antineoplastic drugs in aqueous solutions using Raman spectroscopy. Eur J Pharm Sci. janv 2018;111:158-66.
8. Sharma B, Frontiera RR, Henry A-I, Ringe E, Van Duyne RP. SERS: Materials, applications, and the future. Mater Today. 2012;15(1-2):16-25.
9. Kneipp K, Kneipp H, Manoharan R, Itzkan I, Dasari RR, Feld MS. Near-infrared surface-enhanced Raman scattering can detect single molecules and observe 'hot' vibrational transitions. J Raman Spectrosc. 1998;29(8):743-7.
10. Cailletaud J, De Bleye C, Dumont E, Sacré P-Y, Netchacovitch L, Gut Y, et al. Critical review of surface-enhanced Raman spectroscopy applications in the pharmaceutical field. J Pharm Biomed Anal. 5 janv 2018;147:458-72.
11. Goodacre R, Graham D, Faulds K. Recent developments in quantitative SERS: Moving towards absolute quantification. TrAC Trends Anal Chem. 1 mai 2018;102:359-68.
12. Muhamadali H, Watt A, Xu Y, Chisanga M, Subaihi A, Jones C, et al. Rapid Detection and Quantification of Novel Psychoactive Substances (NPS) Using Raman Spectroscopy and Surface-Enhanced Raman Scattering. Front Chem [Internet]. 2019 [cité 29 mai 2021];7. Disponible sur: https://www.frontiersin.org/articles/10.3389/fchem.2019.00412/full
13. Junior BRA, Soares FLF, Ardila JA, Durango LGC, Forim MR, Carneiro RL. Determination of B-complex vitamins in pharmaceutical formulations by surface-enhanced Raman spectroscopy. Spectrochim Acta A Mol Biomol Spectrosc. 5 janv 2018;188:589-95.
14. Markina NE, Goryacheva IYu, Markin AV. Sample pretreatment and SERS-based detection of ceftriaxone in urine. Anal Bioanal Chem. mars 2018;410(8):2221-7.
15. Alharbi O, Xu Y, Goodacre R. Simultaneous multiplexed quantification of caffeine and its major metabolites theobromine and paraxanthine using surface-enhanced Raman scattering. Anal Bioanal Chem. 2015;407(27):8253-61.
16. De Bleye C, Dumont E, Rozet E, Sacré P-Y, Chavez P-F, Netchacovitch L, et al. Determination of 4-aminophenol in a pharmaceutical formulation using surface enhanced Raman scattering: From development to method validation. Talanta. 15 nov 2013;116:899-905.
17. Alharbi O, Xu Y, Goodacre R. Detection and quantification of the opioid tramadol in urine using surface enhanced Raman scattering. Analyst. 10 août 2015;140(17):5965-70.
18. Dowek A, Lê LMM, Rohmer T, Legrand F-X, Remita H, Lampre I, et al. A

mathematical approach to deal with nanoparticle polydispersity in surface enhanced Raman spectroscopy to quantify antineoplastic agents. Talanta. 1 sept 2020;217:121040.
19. Fan M, Andrade GF, Brolo AG. A review on the fabrication of substrates for surface enhanced Raman spectroscopy and their applications in analytical chemistry. Anal Chim Acta. 2011;693(1-2):7-25.
20. Turkevich J, Stevenson PC, Hillier J. A study of the nucleation and growth processes in the synthesis of colloidal gold. Discuss Faraday Soc. 1 janv 1951;11(0):55-75.
21. Lee PC, Meisel D. Adsorption and surface-enhanced Raman of dyes on silver and gold sols. J Phys Chem. 1982;86(17):3391-5.
22. Shi L, Buhler E, Boué F, Carn F. How does the size of gold nanoparticles depend on citrate to gold ratio in Turkevich synthesis? Final answer to a debated question. J Colloid Interface Sci. avr 2017;492:191-8.
23. Li W, Zhao X, Yi Z, Glushenkov AM, Kong L. Plasmonic substrates for surface enhanced Raman scattering. Anal Chim Acta. 2017;984:19-41.
24. Tian F, Bonnier F, Casey A, Shanahan AE, Byrne HJ. Surface enhanced Raman scattering with gold nanoparticles: effect of particle shape. Anal Methods. 2014;6(22):9116-23.
25. Fisk H, Westley C, Turner NJ, Goodacre R. Achieving optimal SERS through enhanced experimental design: Achieving SERS by enhanced experimental design. J Raman Spectrosc. janv 2016;47(1):59-66.
26. Cailletaud J, De Bleye C, Dumont E, Sacré P-Y, Gut Y, Leblanc N, et al. Detection of low dose of piroxicam polymorph in pharmaceutical tablets by surface-enhanced Raman chemical imaging (SER-CI) and multivariate analysis. Int J Pharm. 3 déc 2019;118913.
27. Eliasson C, Lorén A, Murty KVGK, Josefson M, Käll M, Abrahamsson J, et al. Multivariate evaluation of doxorubicin surface-enhanced Raman spectra. Spectrochim Acta A Mol Biomol Spectrosc. 1 août 2001;57(9):1907-15.
28. Deng B, Luo X, Zhang M, Ye L, Chen Y. Quantitative detection of acyclovir by surface enhanced Raman spectroscopy using a portable Raman spectrometer coupled with multivariate data analysis. Colloids Surf B Biointerfaces. 1 janv 2019;173:286-94.
29. Weng S, Yu S, Dong R, Zhao J, Liang D. Detection of Pirimiphos-Methyl in Wheat Using Surface-Enhanced Raman Spectroscopy and Chemometric Methods. Mol Basel Switz. 30 avr 2019;24(9).
30. Dijkstra RJ, Scheenen WJJM, Dam N, Roubos EW, ter Meulen JJ. Monitoring neurotransmitter release using surface-enhanced Raman spectroscopy. J Neurosci Methods. janv 2007;159(1):43-50.
31. Moody AS, Sharma B. Multi-metal, Multi-wavelength Surface-Enhanced Raman Spectroscopy Detection of Neurotransmitters. ACS Chem Neurosci. 20 juin 2018;9(6):1380-7.
32. Shi C-X, Chen Z-P, Chen Y, Liu Q, Yu R-Q. Quantification of dopamine in biological samples by surface-enhanced Raman spectroscopy: Comparison of different calibration models. Chemom Intell Lab Syst. oct 2017;169:87-93.
33. Hubert Ph, Nguyen-Huu J-J, Boulanger B, Chapuzet E, Chiap P, Cohen N, et al. Harmonization of strategies for the validation of quantitative analytical procedures: A SFSTP proposal – Part II. J Pharm Biomed Anal. 21 sept 2007;45(1):70-81.
34. Eilers PHC, Boelens HFM. Baseline Correction with Asymmetric Least Squares Smoothing. :24.
35. Olivieri AC. Practical guidelines for reporting results in single-and multi-component analytical calibration: a tutorial. Anal Chim Acta. 2015;868:10-22.
36. Wold S, Sjöström M, Eriksson L. PLS-regression: a basic tool of chemometrics. Chemom Intell Lab Syst. 28 oct 2001;58(2):109-30.
37. Barker M, Rayens W. Partial least squares for discrimination. J Chemom. 24 mars 2003;17(3):166-73.

38. Lee NSoo, Hsieh YZung, Paisley RF, Morris MD. Surface-enhanced Raman spectroscopy of the catecholamine neurotransmitters and related compounds. Anal Chem. mars 1988;60(5):442-6.
39. Moody AS, Baghernejad PC, Webb KR, Sharma B. Surface Enhanced Spatially Offset Raman Spectroscopy Detection of Neurochemicals Through the Skull. Anal Chem. 6 juin 2017;89(11):5688-92.
40. Munro CH, Smith WE, Garner M, Clarkson J, White PC. Characterization of the surface of a citrate-reduced colloid optimized for use as a substrate for surface-enhanced resonance Raman scattering. Langmuir. 1995;11(10):3712-20.
41. Park J-W, Shumaker-Parry JS. Structural Study of Citrate Layers on Gold Nanoparticles: Role of Intermolecular Interactions in Stabilizing Nanoparticles. J Am Chem Soc. 5 févr 2014;136(5):1907-21.
42. Moody AS, Payne TD, Barth BA, Sharma B. Surface-enhanced spatially-offset Raman spectroscopy (SESORS) for detection of neurochemicals through the skull at physiologically relevant concentrations. The Analyst. 2020;145(5):1885-93.
43. Moody AS, Sharma B. Multi-metal, Multi-wavelength Surface-Enhanced Raman Spectroscopy Detection of Neurotransmitters. ACS Chem Neurosci. 20 juin 2018;9(6):1380-7.
44. Vander Ende E, Bourgeois MR, Henry A-I, Chávez JL, Krabacher R, Schatz GC, et al. Physicochemical Trapping of Neurotransmitters in Polymer-Mediated Gold Nanoparticle Aggregates for Surface-Enhanced Raman Spectroscopy. Anal Chem. 6 août 2019;91(15):9554-62.